

The thickness of a liquid layer on the free surface of ice as obtained from computer simulation

M. M. Conde,¹ C. Vega,^{1,a)} and A. Patrykiewicz²

¹*Departamento de Química Física, Facultad de Ciencias Químicas, Universidad Complutense, 28040 Madrid, Spain*

²*Faculty of Chemistry, MCS University, 20031 Lublin, Poland*

(Received 11 January 2008; accepted 16 May 2008; published online 1 July 2008)

Molecular dynamic simulations were performed for ice I_h with a free surface by using four water models, SPC/E, TIP4P, TIP4P/Ice, and TIP4P/2005. The behavior of the basal plane, the primary prismatic plane, and of the secondary prismatic plane when exposed to vacuum was analyzed. We observe the formation of a thin liquid layer at the ice surface at temperatures below the melting point for all models and the three planes considered. For a given plane it was found that the thickness of a liquid layer was similar for different water models, when the comparison is made at the same undercooling with respect to the melting point of the model. The liquid layer thickness is found to increase with temperature. For a fixed temperature it was found that the thickness of the liquid layer decreases in the following order: the basal plane, the primary prismatic plane, and the secondary prismatic plane. For the TIP4P/Ice model, a model reproducing the experimental value of the melting temperature of ice, the first clear indication of the formation of a liquid layer, appears at about -100 °C for the basal plane, at about -80 °C for the primary prismatic plane, and at about -70 °C for the secondary prismatic plane. © 2008 American Institute of Physics.

[DOI: 10.1063/1.2940195]

I. INTRODUCTION

The hypothesis of the formation of a liquidlike layer on the surface of ice at temperatures below the bulk melting point temperature has been the subject of intermittent controversy since it was first proposed by Faraday.¹ It is now commonly accepted that melting starts at the surface and solids exhibit a liquidlike layer at the surface, already at the temperatures lower than the bulk melting point.^{2–10} When the thickness of that liquid layer diverges at the melting point, the melting is denoted as surface melting. When the thickness of the liquid layer remains finite at the melting point this is denoted as incomplete surface melting.^{11–13} The thickness of a quasiliquid layer at a given temperature depends on the material considered and on the crystallographic plane exposed (as labeled by the Miller indexes). Whenever the thickness of a liquid layer is sufficiently large, either because the system undergoes a surface melting or an incomplete surface melting (with a significantly thick liquid layer), it is not possible to superheat a solid. Due to the ubiquitous character of water, it is of particular interest to determine the structure of the surface of ice^{14–17} and, in particular, the structure of a water liquid layer on ice at the temperatures below the melting point. The solution to that problem is not only important from a fundamental point of view but also from a practical point of view. The existence of a liquid layer of water on the free surface of ice at temperatures below the melting point (usually denoted as a quasiliquid water to illustrate the point that although liquid in character it is not fully equivalent to bulk water) is relevant to describe differ-

ent phenomena. For instance, it is one of the explanations provided to understand why it is so easy to skate on ice,¹⁸ although frictional heating is also playing an important role.^{19,20} Also it has been suggested that the existence of a liquid layer on ice may play an important role in chemical reactions occurring in the stratospheric clouds leading to the annual depletion of ozone in the Antarctic region.²¹ Thus, a number of important problems are connected in one way or another to the existence of such a liquid water layer at the ice surface and that explain the appearance of several review papers that have appeared recently.^{22–24}

Is there any evidence of the existence of a quasiliquid water layer on the free surface of ice? Yes, all experiments point out to the existence of such a quasiliquid water layer.^{25–31} Unfortunately there is no consensus about its thickness. In fact, the thickness of such layers may differ by an order of magnitude (sometimes almost by two) depending on the technique used.^{22,23} The problem is certainly difficult and to understand the origin of these discrepancies further work is still needed. Therefore, it is of interest to see if quasiliquid layers of water are also observed in computer simulations. It is the main goal of this work to investigate this problem.

When performing computer simulations of ice, it is necessary to choose a model of water. If the goal of the simulations is to establish the existence of a quasiliquid water layer at temperatures below the melting point, it is absolutely needed to know the melting point of the different water models. Some of the most popular water models, as TIP3P,³² TIP4P,³² and SPC/E,³³ which are now used in computer simulations on a routine basis, were proposed in the early

^{a)}Electronic mail: cvega@quim.ucm.es.

1980s. Somewhat surprisingly the melting points were not established on a firm basis, and only the pioneering work of Haymet and co-workers,^{34,35} Gay and Smith,³⁶ Bryk and Haymet,³⁷ and Gao *et al.*³⁸ provided the first reasonable estimates of the melting point of ice Ih for these models. These early values of the melting temperature were about 10 K above the current estimate of the ice melting point.^{39–44} Fortunately, the melting points of TIP4P and SPC/E models have been established on a firm basis over the last three years, being equal to 230(3) and 215(4) K, respectively.^{36,37,39–46} Free energy calculations performed by our group in Madrid^{39,41,45} and by Koyama *et al.*⁴⁰ are consistent with the quoted values. Besides, direct simulations of the ice-liquid water coexistence, done by our group,⁴² by Vrba and Jungwirth,⁴⁶ and by Wang *et al.*,⁴³ have also confirmed those values of the melting point temperature. It is clear that for these two models the melting point is rather low as compared to the experimental value. It should be emphasized that not only the melting points but also complete phase diagrams have been determined for these models. It has been shown that the TIP4P model is superior to SPC/E in describing the global phase diagram of water.³⁹ For this reason, we have modified slightly the parameters of the original TIP4P model to reproduce either the experimental value of the melting point, named TIP4P/Ice model, or to reproduce the temperature of maximum density of the liquid at the room pressure isobar, the model named TIP4P/2005.⁴⁷ The melting points of TIP4P/Ice and TIP4P/2005 models are of 271(3) and 249(3) K, respectively. Once the melting point of these models is established firmly it seems a proper moment to analyze the existence of a quasiliquid water layer at the temperatures below the melting point. The interest in determining the existence of a quasiliquid water layer is growing enormously in recent years, following the pioneering works of Kroes⁴⁸ and of Furukawa and Nada.^{49,50} In fact, in the last three years several groups have analyzed this issue in detail. Carignano *et al.*⁵¹ and Ikeda-Fukazawa and Kawamura⁵² have clearly shown the existence of the quasiliquid water layer for two different water models. Carignano *et al.*⁵³ have also studied the effect on impurities (NaCl) on the quasiliquid layer using the TIP6P model of water proposed by Nada and van der Eerden.⁵⁴ Quantum effects on the quasiliquid layer have also been considered by Paesani and Voth⁵⁵ in a recent study. The behavior of a thin film of ice I deposited on MgO has been studied in detail by Picaud.⁵⁶ Also we have recently reported⁵⁷ the existence of the liquid layer for TIP4P, SPC/E, TIP4P/Ice, and TIP4P/2005 models. In our recent work^{57,58} it has been shown that superheating of ice Ih is suppressed by the existence of a free surface, since the existence of such a free surface induces the formation of a quasiliquid layer, thus reducing to zero the activation energy of the formation of liquid nucleus,^{59,60} as first speculated by Frenkel.⁶¹ Besides we have shown recently that the study of the free surface provides a new methodology to estimate the melting point of water models. In fact, the melting point temperature obtained from our simulations of the free surface was fully consistent with the values obtained by other routes and by different authors. If the emphasis of our previous work⁵⁷ was to propose a new methodology to estimate the melting point of

water models and to show the absence of superheating of ice with a free surface, in this work we focus on the study of quasiliquid water layer and its thickness, using different water models and different free surfaces of ice.

II. METHODOLOGY

Although the ice I_h is hexagonal, it is possible to use an orthorhombic unit cell.⁶² It was with this orthorhombic unit cell that we generated the initial slab of ice. In ice I_h , protons are disordered while still fulfilling the Bernal–Fowler rules.^{63,64} We used the algorithm of Buch *et al.*⁶⁵ to obtain an initial configuration with proton disorder and almost zero dipole moment (less than 0.1 Debye) and satisfying the Bernal–Fowler rules. In order to equilibrate the solid, *NPT* simulations of bulk ice I_h were performed at zero pressure for each temperature considered. We used the molecular dynamics (MD) package GROMACS (version 3.3).⁶⁶ The time step was 1 fs and the geometry of the water molecules was enforced using constraints.^{67,68} The Lennard-Jones potential was truncated at 9.0 Å. Ewald sums were used to deal with electrostatics. The real part of the Coulombic potential was truncated at 9.0 Å. The Fourier part of the Ewald sums was evaluated by using the particle mesh Ewald (PME) method of Essmann *et al.*⁶⁹ The width of the mesh was 1 Å, and we used a fourth order polynomial. The temperature was kept by using a Nosé–Hoover^{70,71} thermostat with a relaxation time of 2 ps. To keep the pressure constant, a Parrinello–Rahman barostat,^{72,73} with all three sides of the simulation box were allowed to fluctuate independently, was used. The relaxation time of the barostat was of 2 ps. The pressure of the barostat was set to zero. The angles were kept orthogonal during this *NPT* run, so that they were not modified with respect to the initial configuration. The use of a barostat allowing for independent fluctuations of the lengths of the simulation box sides is important. In this way, the solid can relax to equilibrium by adjusting the unit cell size and shape for the considered model and thermodynamic conditions. It is not a good idea to impose the geometry of the unit cell. The system should rather determine it from *NPT* runs. Once the ice is equilibrated at zero pressure we proceed to generate the ice-vacuum interface. By convention, we shall assume in this paper that the x axis is perpendicular to the ice-vacuum interface. The ice-vacuum configuration was prepared by simply changing the box dimension along the x axis, from the value obtained from the *NPT* simulations of bulk ice to a much larger value. The size of the simulation in the y and z dimensions was not modified. In other words, a slab of ice was located in the middle of a simulation box, and periodic boundary conditions were used in the three directions of space. The size of the box in the x direction was about three times larger than the size of the ice in the y and z directions, so that it is expected that the results obtained are not affected by the interaction of the ice with its periodical image.

Three different planes were used here as the free ice-vacuum interface. First, the secondary prismatic plane (i.e., the $1\bar{2}10$ plane) was considered. In this case we used 1024 molecules, and the approximate size of the simulation box was of $100 \times 31 \times 29$ Å³ (the sizes of the cell in both the y

TABLE I. Details of the geometry of the initial configuration for different planes of ice corresponding to different water models. L_x , L_y , L_z are the dimensions of the simulation box in Å. The x axis is perpendicular to the ice-vacuum interface. L_{ice} is the size of the initial block of ice (in the x direction). All dimensions are given in Å.

N	The plane exposed	L_x	L_y	L_z	L_{ice}
1024	Secondary prismatic	100	31	29	36
1536	Basal	110	31	27	59
1536	Primary prismatic	110	30	27	62

and z directions are only approximate since the actual values were obtained from the *NPT* runs at zero pressure for each water model and temperature). The approximate area of the ice-vacuum interface was about $31 \times 29 \text{ \AA}^2$. This is about ten molecular diameters in each direction parallel to the interface. Although the interface properties present important finite size effects,⁷⁴ there is a certain consensus about the fact that ten molecular diameters provide reliable estimates of the surface tension of the vapor-liquid interface for water and other systems, and it seems reasonable to expect that the same is true for the ice-vacuum interface.⁷⁵

We have also analyzed the behavior of ice, when the plane exposed to vacuum was the basal plane. In this case we used 1536 molecules and the dimensions of the simulation box were $110 \times 31 \times 27 \text{ \AA}^3$ (approximately since the y and z values were slightly different for each water model and temperature). Finally we have also considered the prismatic primary plane. In this case, we used 1536 molecules, and the dimensions of the simulation box were $110 \times 30 \times 27 \text{ \AA}^3$. In Table I, the details of the geometry of the initial configuration are summarized.

More details regarding the relation of the main planes of ice (basal, primary prismatic, and secondary prismatic) to the hexagonal unit cell can be found in Fig. 1 of the paper by Nada and Furukawa,⁷⁶ in the paper by Carignano *et al.*,⁵¹ and also at the water website of Chaplin.⁷⁷ Let us just mention that when an orthorhombic unit cell of ice Ih is used, the faces of the unit cell are just the secondary prismatic plane, the primary prismatic plane, and the basal plane. Hexagons are clearly visible when the crystal is looked at from the basal plane and from the secondary prismatic plane, but not when it is viewed from the side of primary prismatic plane. In the basal plane one of the sides of the hexagons is parallel to the edge where the basal and the secondary prismatic planes intersect (this is not true for the secondary prismatic plane) providing a simple way to distinguish the basal and the secondary prismatic planes.

Once the ice-vacuum system was prepared, we performed relatively long *NVT* runs (the lengths were between 6 and 12 ns depending on the water model and thermodynamic conditions). Since we have been using *NVT* MD, the dimensions of the simulation box have been fixed, of course, unlike in the preceding *NPT* run. During this *NVT* simulations, configurations were stored for further analysis every 4–8 ps, after an equilibration period of about 2 ns. Thus, typically at the end of a run, about 1500 independent configurations were available for analysis.

Once the simulations were performed we could proceed to analyze the configurations obtained. Since the purpose of

this study is to determine the liquid layer thickness at the free surface of ice, a criterion allowing to distinguish liquidlike and icelike molecules is needed. We should admit from the very beginning that there is not a unique procedure to do that. Mapping a configuration (with a continuous set of coordinates of the molecules) into a discrete set, i.e., the numbers of liquidlike and icelike molecules requires to establish the borders between the two phases. Also, going from a configuration of water molecules (with a continuous set of coordinates of the molecules) to a number of hydrogen bonds requires a somewhat arbitrary definition of the hydrogen bond. Not surprisingly papers appear almost every year providing a new definition of the hydrogen bond, and therefore give different estimations of the hydrogen bonds present in water.⁷⁸ Our approach here is to establish a reasonable criterion to distinguish liquidlike from icelike molecules in a given configuration. We do hope that this allows for a qualitative discussion of the results and a progress in the field. We admit that different definitions of icelike and liquidlike molecules may yield different results than reported here, but the qualitative discussion would remain very much the same. We do really doubt that an absolute, nonarbitrary definition of what is liquidlike and icelike parts of the system does exist when one deals with a problem in which both phases are in contact, as it is the case of the free surface of ice. To define icelike and liquidlike molecules we shall use the tetrahedral order parameter first introduced by Errington and Debenedetti⁷⁹ and that was found quite useful to describe the structure of glassy water.⁸⁰ For each molecules (i), this parameter q_i is defined as

$$q_i = \left[1 - \frac{3}{8} \sum_{j=1}^3 \sum_{k=j+1}^4 \left(\cos(\theta_{j,i,k}) + \frac{1}{3} \right)^2 \right], \quad (1)$$

where the sum is over the four nearest neighbors (oxygens) of the oxygen of the i th water molecule. The angle $\theta_{j,i,k}$ is the angle formed by the oxygens of molecules j , i , and k (being molecule i the vertex of the angle). The tetrahedral order parameter adopts a value of 1, when the four nearest neighbors adopt a tetrahedral arrangement around the central one. Notice that negative values of q are also possible when the four nearest neighbors adopt a linearlike configuration. Let us define $p(q)$, the probability density $p(q)$, as

$$p(q) = \left\langle \frac{N(q)}{N\Delta q} \right\rangle, \quad (2)$$

where $N(q)$ is the number of molecules in a given configuration having an order parameter between q and $q + \Delta q$, with Δq being the size of the grid. The total number of molecules

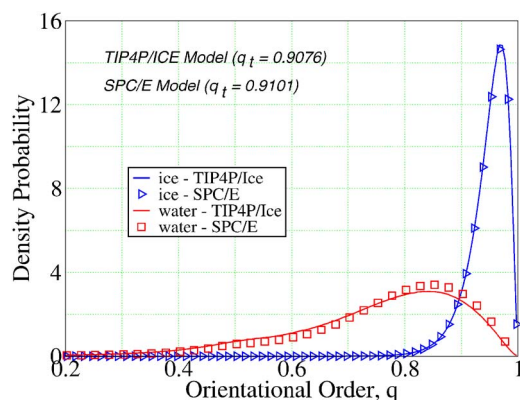


FIG. 1. (Color online) Probability density distribution $p(q)$ of the orientational order parameter q , for the water models TIP4P/Ice and SPC/E as obtained at the melting point temperature of the models (at room pressure) from simulations of bulk water and bulk ice Ih. Results for TIP4P and TIP4P/2005 (not shown) were almost indistinguishable from those of the TIP4P/Ice model.

in the system is denoted as N . The brackets in the above equation mean an ensemble average. Obviously the probability density $p(q)$ is normalized to unity so that

$$1 = \int p(q) dq. \quad (3)$$

We have analyzed the distribution function of the order parameter q , in pure ice $p_{\text{Ih}}(q)$ and in pure liquid $p_{\text{liquid}}(q)$. For that purpose independent simulations were performed for bulk water and bulk ice. In Fig. 1, the distributions $p(q)$ are presented for the TIP4P/Ice and SPC/E water models. The results were obtained at the respective melting point temperatures. As it is seen, the results for these models are quite similar (when they are compared at their respective melting point temperatures). For the ice Ih the distribution of $p(q)$ is rather narrow and centered around 0.98, whereas the distribution for water is broader and centered around 0.85. Not surprisingly there is a significant amount of tetrahedral order in liquid water at the melting point temperature. Certainly our results provide further evidence⁸¹ of the existence of tetrahedral order in liquid water in spite of certain claims challenging this point of view.⁸² The distributions for liquid water obtained by us are in agreement with those presented recently by Jhon *et al.*⁸³ for liquid water. The two distributions, $p_{\text{Ih}}(q)$ and $p_{\text{liquid}}(q)$, exhibit a certain degree of overlap. We shall define a threshold value for q , i.e., q_t so that if the value of q of a given molecule is larger than q_t the molecule is considered as being icelike, while for the value of q smaller than q_t it is considered as a liquidlike. The threshold value will be obtained for each model from the relation

$$\int_{q_t}^1 p_{\text{liquid}}(q) dq = \int_0^{q_t} p_{\text{Ih}}(q) dq, \quad (4)$$

where $\int_{q_t}^1 p_{\text{liquid}}(q) dq$ is the probability of incorrectly assigning an liquidlike as icelike and $\int_0^{q_t} p_{\text{Ih}}(q) dq$ is the probability of incorrectly assigning an icelike as liquidlike. In other words, the threshold value q_t is the value of q at which the area of $p_{\text{liquid}}(q)$ (for values of q larger than q_t) is equal to the area under the curve $p_{\text{Ih}}(q)$ (for values of q smaller than q_t).

TABLE II. Threshold value of the orientational order parameter q_t for the different water models (as determined at their respective melting temperatures).

Model	q_t
TIP4P/Ice	0.9076
TIP4P/2005	0.9085
TIP4P	0.9105
SPC/E	0.9101

So, by equating the probability of incorrectly assigning, the errors cancel out. For the threshold value there are as many water molecules having a value of q larger than q_t as molecules of ice Ih having a value of q smaller than q_t . The threshold values for different water models at the melting point temperature are given in Table II. As it is seen the threshold value of q is practically identical for all water models. For this reason the value $q_t=0.91$ will be used hereafter for all water models. In a given configuration a molecule will be labeled as a liquidlike whenever the value of q is smaller than $q_t=0.91$ and will be classified as an icelike whenever its value of q is larger than $q_t=0.91$. Notice that q_t is close to (but not identical with) the point where $p_{\text{liquid}}(q)$ and $p_{\text{Ih}}(q)$ intersect.

III. RESULTS AND DISCUSSION

We shall start with the presentation of results for the TIP4P/Ice model. In Fig. 2 the instantaneous number of liquidlike molecules is presented as a function of the simulation time for the TIP4P/Ice model. The results correspond to the case in which the secondary prismatic plane is exposed to vacuum. It is quite evident that the number of liquidlike molecules increases significantly with temperature and fluctuates around the corresponding average values. The fluctuations increase with temperature as well.

The thickness of the liquidlike layer has been estimated as follows:

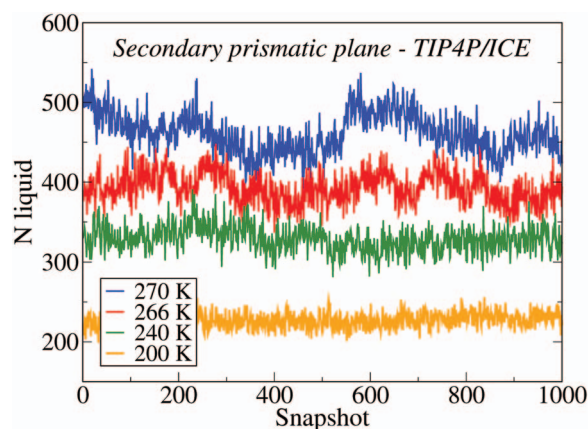


FIG. 2. (Color) Instantaneous number of liquid molecules N_{liquid} as a function of the simulation time for the TIP4P/Ice model (secondary prismatic plane).

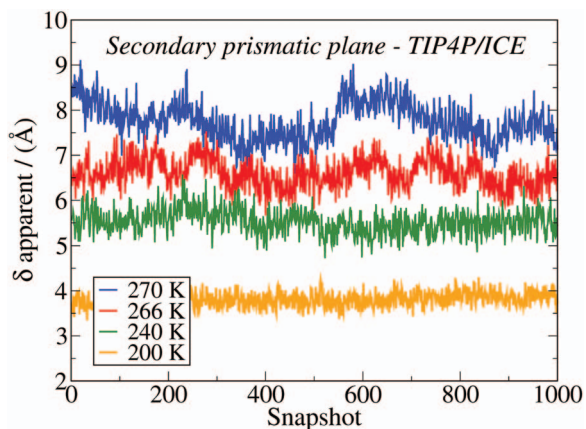


FIG. 3. (Color) Instantaneous values of the liquid layer thickness δ_{apparent} as a function of the simulation time for the TIP4P/Ice model (secondary prismatic plane).

$$\delta_{\text{apparent}}(\text{\AA}) = \frac{N_{\text{liquid}}M}{2\rho N_{\text{AV}}L_yL_z10^{-24}}, \quad (5)$$

where N_{liquid} is the average number of liquidlike molecules along the run, M is the molecular weight of water (18.015 74 g/mol), N_{AV} is Avogadro's number, the product of L_y and L_z is the area of the interface when both lengths are given in angstroms, 10^{-24} is the factor needed to convert cm^3 to \AA^3 , while ρ is the density of liquid water in g/cm^3 . The factor of 2 appears in the denominator of the above equation due to the fact that the ice block exhibits two identical inter-

TABLE III. Thickness of the liquid layer for different planes of the TIP4P/Ice model. δ_{apparent} and δ_{true} are given in \AA and the temperature is given in K.

Water model and plane	T	δ_{apparent}	δ_{true}	
TIP4P/Ice (Secondary prism.)	270	7.3(5)	4.4(7)	
	269	7.2(5)	4.3(7)	
	266	6.7(3)	3.8(5)	
	264	6.6(4)	3.7(6)	
	250	5.6(3)	2.7(5)	
	230	4.6(2)	1.7(4)	
	200	3.9(3)	1.0(5)	
	170	3.4(2)	0.5(4)	
	150	3.2(2)	0.3(4)	
	123	3.1(2)	0.2(4)	
TIP4P/Ice (Basal)	30	2.9(2)	0.0(2)	
	270	9.6(5)	7.5(7)	
	268	9.6(5)	7.5(7)	
	266	8.4(2)	6.3(4)	
	240	5.9(3)	3.8(5)	
	200	4.1(2)	2.0(4)	
	170	3.3(2)	1.2(4)	
	30	2.1(2)	0.0(2)	
	TIP4P/Ice (Primary prism.)	270	9.5(6)	6.8(8)
		268	9.0(6)	6.3(8)
266		8.5(6)	5.8(8)	
240		5.4(3)	2.7(5)	
200		4.0(2)	1.3(4)	
30		2.7(2)	0.0(2)	

TABLE IV. Thickness of the liquid layer for the different water models (TIP4P/2005, TIP4P, and SPC/E). δ_{apparent} and δ_{true} are given in \AA and the temperature is given in K.

Water model and plane	T	δ_{apparent}	δ_{true}
TIP4P/2005 (Secondary prism.)	249	8.5(1.0)	6.0(1.2)
	247	7.3(4)	4.8(6)
	245	6.8(3)	4.3(5)
	244	6.7(4)	4.2(6)
	230	5.3(3)	2.8(5)
	200	4.1(2)	1.6(4)
	180	3.8(2)	1.3(4)
	140	3.4(2)	0.9(4)
	100	3.0(2)	0.5(4)
	30	2.5(2)	0.0(2)
TIP4P (Secondary prism.)	228	7.1(4)	4.6(6)
	224	6.6(3)	4.1(5)
	200	3.9(2)	1.4(4)
	160	3.8(2)	1.3(4)
	30	2.5(2)	0.0(2)
SPC/E (Secondary prism.)	212	7.0(2)	4.0(4)
	209	6.3(5)	3.3(7)
	150	4.1(2)	1.1(4)
	30	3.0(2)	0.0(2)

faces, one appearing on the left side and the other on the right side of the simulation cell. As already mentioned, the values of L_y and L_z change slightly from one model to another and from one temperature to another. To compute the liquid layer thickness we shall neglect these small variations and we always use the values reported in Table I. Concerning the density of water, which appear in the denominator of Eq. (5), it also changes from one water model to another and with the temperature. However, for the water models considered in this work the density of water at the melting point⁴⁴ is close to $0.99 \text{ g}/\text{cm}^3$. For this reason we shall use this value to estimate the liquid layer thickness δ_{apparent} . The origin of the subscript ‘‘apparent’’ will be clarified later on. In summary, the thickness of a liquid layer is obtained by equating the average number of liquidlike molecules obtained from the simulation of the free interface to that of a sample of pure water of dimensions $L_y L_z \delta_{\text{apparent}}$.

The instantaneous values (along the run) of the liquid layer thickness of the secondary prismatic plane of the TIP4P/Ice model are presented in Fig. 3. As it is seen, the fluctuations of about 1 \AA in the liquid layer thickness are clearly visible along the run at the highest temperature, whereas these fluctuations are much smaller at the lowest temperature.

In Table III the thickness of the liquid layer, δ_{apparent} , as a function of temperature is reported for the secondary prismatic plane. Results are presented from very low temperatures to temperatures quite close to the melting point. A somewhat surprising result is that the value of the liquid layer thickness is not zero even at a temperature as low as 30 K. An inspection of snapshots from the simulations at that temperature reveals the absence of a liquid layer. One has to ask the question: Why is the number of liquid molecules and

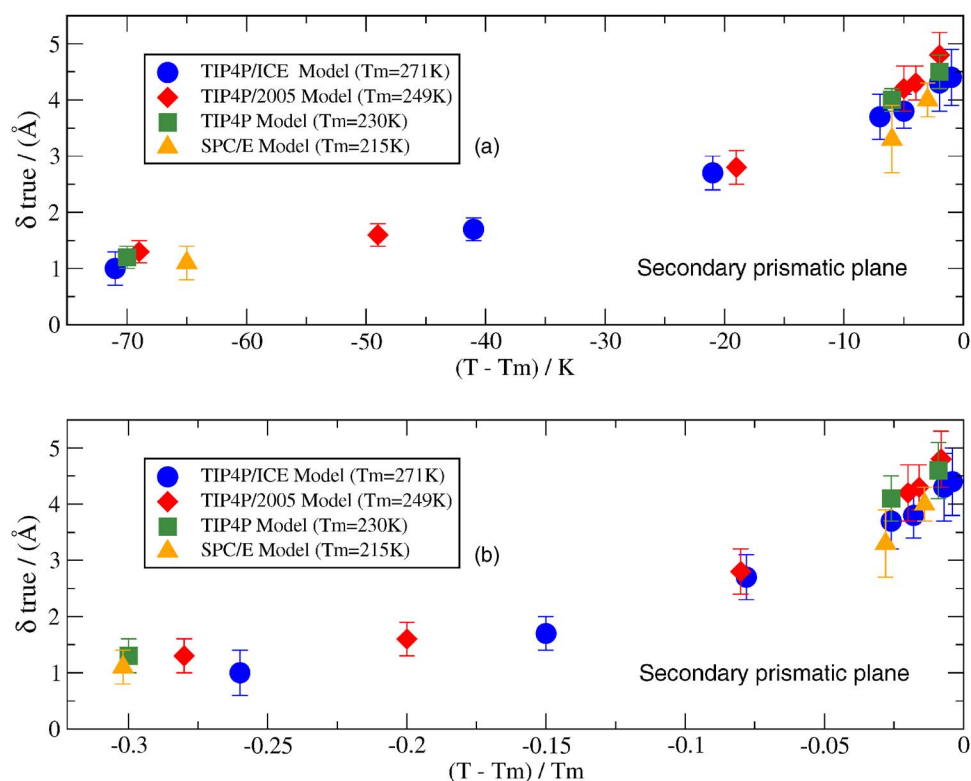


FIG. 4. (Color online) The Thickness of a liquid layer for the secondary prismatic plane as a function of the undercooling (a) and of the reduced undercooling (b) of the model for the different models of water potentials.

hence the thickness of a liquid layer nonzero at 30 K? The reason is that our definition of q involves the four nearest neighbors of each molecule. For the molecules occupying the very last layer of ice it is not possible to form four hydrogen bonds²² (so that at least one of the four nearest neighbors is not located in a tetrahedral way). Therefore, the value of q for the molecules occupying the last layer is rather low, and hence such molecules are (incorrectly) classified as liquid-like. For this reason we found it more convenient to define the true liquid layer thickness as

$$\delta_{\text{true}}(T) = \delta_{\text{apparent}}(T) - \delta_{\text{apparent}}(T = 30 \text{ K}), \quad (6)$$

with this definition the liquid layer thickness goes to zero at low temperatures at it should.

Let us now consider the results for other water models. Table IV gives the values of the liquid layer thickness obtained for the TIP4P/2005, TIP4P, and SPC/E models of water. The results reported were obtained for the secondary prismatic plane, and they are similar to those obtained for the TIP4P/Ice model. Notice that the temperatures considered for these models are lower than those analyzed for the TIP4P/Ice model. The reason is that whereas for TIP4P/Ice the melting point reproduces the experimental value, the melting points of TIP4P/2005, TIP4P, and SPC/E models are about 20, 40, and 60 K below the experimental value, respectively. The magnitudes of the liquid layer thickness obtained for the SPC/E, TIP4P, and TIP4P/2005 models are similar to those obtained for the TIP4P/Ice. In Fig. 4 the thickness of the liquid layer at the secondary prismatic plane as a function of the undercooling and of the reduced undercooling is presented for the four water models. It is quite well seen that the results of these water models fall into a unique curve, indicating that there are no significant differences between the

models, when they are compared at the same undercooling or reduced undercooling. In summary it is not a good idea to compare the values of the liquid layer thickness for two different water models, at a given absolute temperature. The liquid layer thickness of two water models should be compared at the same undercooling (in degrees) with respect to the melting point. The results of Fig. 4 manifest clearly that the existence of a liquid layer is not a characteristic feature of one specific water model, but is clearly visible in all models considered in this work. Besides, the results strongly suggest that the thickness of the liquid layer is almost the same for the different water models, when compared at the same relative temperature to the melting point. For this reason in what follows we shall consider only the TIP4P/Ice model, since it is likely that similar results would be obtained with other water models.

In Figs. 5 and 6 the thickness of a liquid layer as ob-

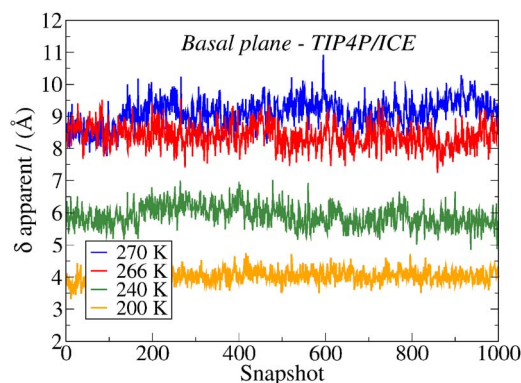


FIG. 5. (Color online) Instantaneous values of the liquid layer thickness δ_{apparent} as a function of the simulation time for the TIP4P/Ice model (basal plane).

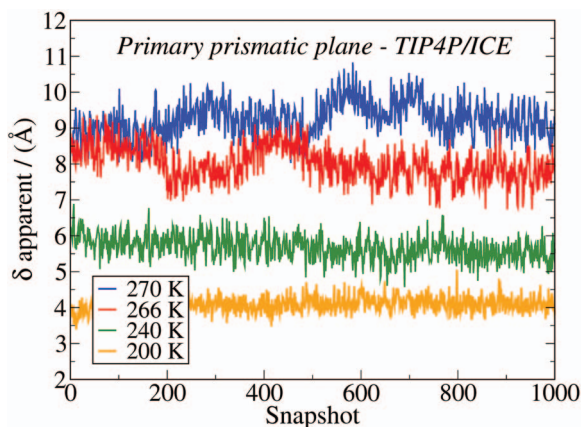


FIG. 6. (Color) Instantaneous values of the liquid layer thickness δ_{apparent} as a function of the simulation time for the TIP4P/Ice model (primary prismatic plane).

tained along the run is presented, when the plane exposed to vacuum is the basal plane and primary prismatic plane, respectively. The results for the liquid layer thickness (both δ_{apparent} and δ_{true}) are summarized in Table III. The first interesting thing to be noted is that at a given temperature the liquid layer thickness adopts the largest value for the basal plane and the smallest one for the secondary prismatic plane. The value of the primary prismatic plane lies between the two. This is more clearly seen in Fig. 7 where the value of δ_{true} for the three planes is plotted as a function of T for the TIP4P/Ice model. An interesting question is the following: at which temperature does the formation of a liquid layer begins? We shall denote this temperature as the premelting temperature. Somewhat arbitrarily (again) we shall define the premelting temperature as this at which δ_{true} adopts the value of 1 Å. In Table V the premelting temperatures for the dif-

ferent water models and different ice planes are presented. The data show that the premelting temperature is located around 70 °C below the melting point for the secondary prismatic plane temperature (this is approximately true for all the considered water models). In the case of the primary prismatic plane, the premelting temperature is located about 80 K below the melting temperature. For the basal plane, however, the premelting starts at a temperature about 100 °C below the melting temperature. It is clear that the basal plane must play a crucial role in the physics of ice, since it is the plane for which the surface melting starts at the lowest temperature and it is the plane for which at a given temperature the thickness of the liquid layer is the largest.

Let us now present the results for density profiles. In Figs. 8–10 the average density profiles for the secondary prismatic plane, the basal plane, and for the primary prismatic plane at three different temperatures are presented. These plots provide a qualitative idea of the number of layers involved in the formation of a liquid film. At low temperatures only the most external layer of water molecules is involved in the formation of a liquid layer. However, at temperatures closer to the melting point two additional ice layers appear as melted. As it is seen each ice layer of the basal plane has a double peak, the first containing three oxygens of the hexagonal ring and the second peak corresponding to the other three oxygens (located at slightly different values of x coordinate). The same is true for the primary prismatic plane. In summary the liquid film involves the first layer of ice at low temperature, and two additional layers at temperatures below (but not too close) to the melting temperatures.

It would be of interest to analyze the scaling behavior of the liquid layer thickness in the vicinity of the melting point (where a divergence may occur). Although such a study has

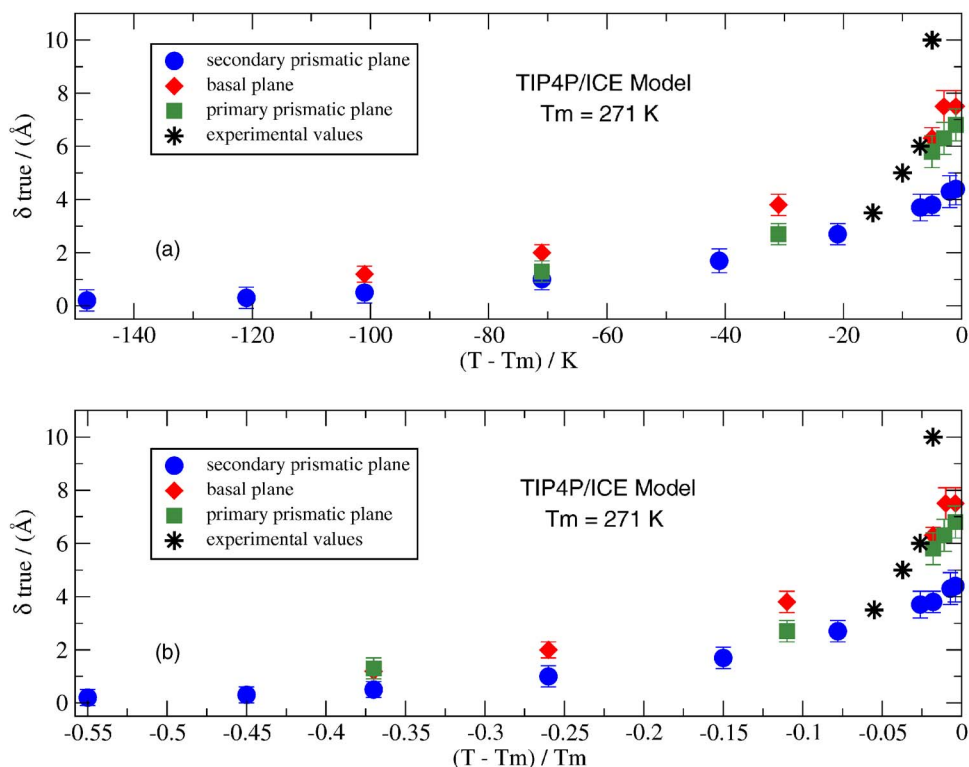


FIG. 7. (Color online) The thickness of a liquid layer for the TIP4P/Ice model at the secondary prismatic, basal, and primary prismatic plane as a function of the undercooling (a) and of the reduced undercooling (b) of the model. Included are the experimental values by Bluhm *et al.* (Ref. 26).

TABLE V. Premelting temperature for different water models and different planes of ice. The temperature is given in K. $T_{\text{pre-melting}}$ is defined as the temperature at which δ_{true} is 1 Å.

Model	T_{melting}	$T_{\text{pre-melting}}$	$T_{\text{pre-melting}} - T_{\text{melting}}$
TIP4P/Ice basal plane	271 (3)	170	~ -100
TIP4P/Ice primary prismatic plane	271 (3)	190	~ -80
TIP4P/Ice secondary prismatic plane	271 (3)	200	~ -70
TIP4P/2005 secondary prismatic plane	249 (3)	180	~ -70
TIP4P secondary prismatic plane	230 (3)	160	~ -70
SPC/E secondary prismatic plane	215 (4)	150	~ -65

not been attempted here, nevertheless it may be of interest in the future. The reason why the study of the divergence may still require further work is twofold. First, it would be necessary to determine the melting point of the different water models with still higher accuracy, reducing the estimated uncertainty by at least one order of magnitude (from 3 K of the current estimates to 0.3 K). Second to analyze the divergence much larger system sizes are required, so that one has a large piece of ice in contact with a liquid layer or rather large area. Roughly speaking, systems sizes of about 20 000 molecules, simulation times of about 100 ns and uncertainty in the melting point temperature of about 0.3 K are needed to analyze the possible divergence of the liquid layer thickness as the melting point is approached.

A different issue is whether the simulation times used in this work (being of the order of several nanoseconds) are sufficiently long to guarantee reliable estimates of the liquid layer thickness. There are two indications suggesting that this is indeed the case. First, the values of the liquid layer thickness exhibit fluctuations around average values, and the value of the average does not tend to increase or decrease with time. Second, the lengths of simulation runs considered in this work are sufficient to melt the block of ice completely, when the temperature is above the melting point. In Fig. 11 the evolution of the potential energy of the system with time is plotted at several temperatures, namely, 300, 290, and 276 K (for the TIP4P/Ice model the melting point of ice Ih is around 271 K). As it can be seen even at the lowest tempera-

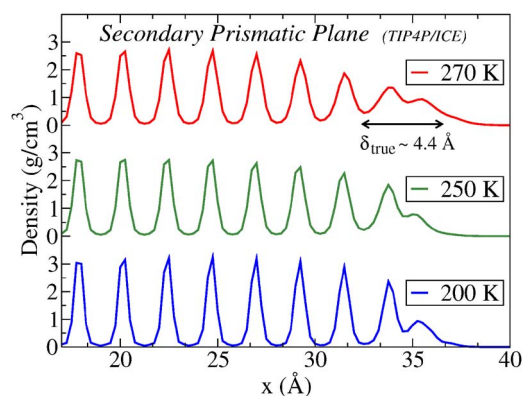


FIG. 8. (Color online) The density profile for the TIP4P/Ice model and the secondary prismatic plane exposed to vacuum.

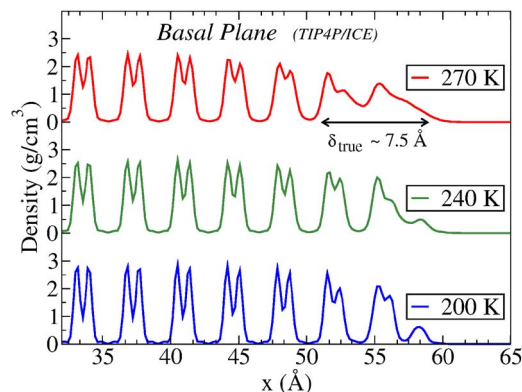


FIG. 9. (Color online) The density profile for the TIP4P/Ice model and the basal plane exposed to vacuum.

ture (276 K) it is possible to melt the ice completely in about 3.5 ns. The final plateau indicates that a complete melting of ice does occur. Obviously, the formation of a liquid layer with a thickness of about 2 or 3 molecular diameter requires less time than a complete melting of the entire ice block. Although the diffusion coefficient is expected to decrease when the temperature becomes lower, we do not expect a dramatic decrease when the temperature drops from say 276 to 266 K. For this reason, a relatively fast melting of the ice block in about 3.5 ns at 276 K strongly suggests that a run of similar length should be enough to obtain a liquid layer thickness of few angstroms. Another indication that the system is well equilibrated is the fact that the average number of liquid molecules is the same for the right and the left interfaces. For the TIP4P/Ice model we have also performed a long run of 30 ns of the secondary prismatic plane at $T = 266$ K, and the liquid layer thickness obtained was almost identical to that obtained from a shorter run of about 8 ns.

Although we have used MD simulations in our study, nevertheless Monte Carlo (MC) simulations could also be used to determine the liquid layer thickness. Motivated by this we have performed NVT MC simulations for the TIP4P/Ice model at the temperatures of 290 and 300 K (both above the melting temperature of the model). MC runs were performed using the same initial configuration as used in MD simulation. The potential was truncated at the same distance, and the rest of the conditions were similar to those of the

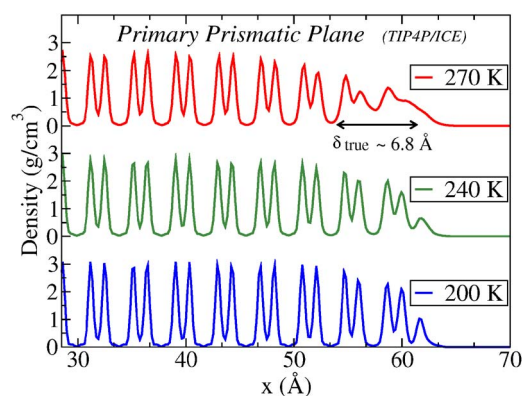


FIG. 10. (Color online) Density profile for the TIP4P/Ice model and the primary prismatic plane exposed to vacuum.

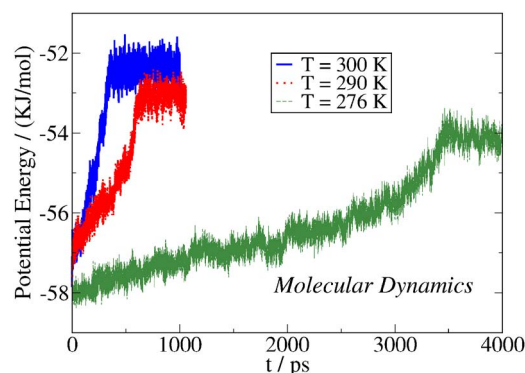


FIG. 11. (Color online) The evolution of the system energy with time at the temperatures of 300, 290, and 276 K for the TIP4P/Ice model obtained by MD simulation. The plane exposed to vacuum was the secondary prismatic plane. The final plateau indicates a complete melting of ice (the temperatures used are above the melting point of the model).

MD simulations (Ewald sums instead of PME were used in this case to deal with the long range electrostatics). The evolution of the energy of the system with the number of steps is presented in Fig. 12 for $T=290$ K. The results are presented so that one MD time step corresponds to a MC cycle (i.e., a trial move per molecule). The figure shows that MC simulation requires about 1.4×10^6 cycles to melt the block of ice completely, while MD simulations (using a thermostat) required only 0.7×10^6 to melt the ice completely. Quite similar results have been obtained at the temperature of 300 K. Not only the value of the melting point temperature but also the thickness of the liquid layer should be the same, regardless of whether it was obtained via MD or MC. In fact, by using our MC program we have determined the liquid layer thickness for the TIP4P/Ice model at $T=250$ K. The length of the run was of 8×10^6 cycles. The value of thickness for the secondary prismatic plane obtained (δ_{apparent}) by MC was of $5.7(3)$ Å which is in complete agreement with the value obtained by MD, i.e., $5.6(3)$ Å. That constitutes a further cross-checking of the results of this work.

It was mentioned in the Introduction that there is a great disparity in the value of the liquid layer thickness obtained by different experimental techniques.^{25–31} In Fig. 7 the thickness of the liquid layer obtained from photoelectron spec-

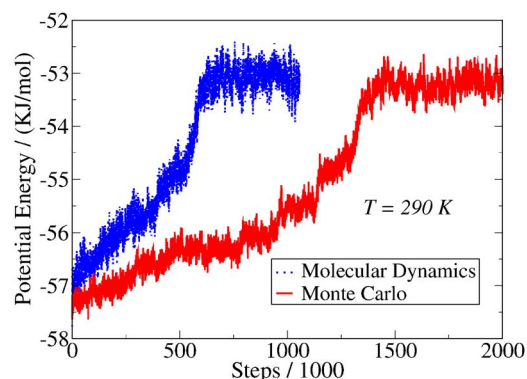


FIG. 12. (Color online) Evolution of the energy of the system with time at 290 K for the TIP4P/Ice model obtained by MD and MC simulations. A single step of MC simulation (a trial move per particle) corresponds to a single time step in MD simulation.

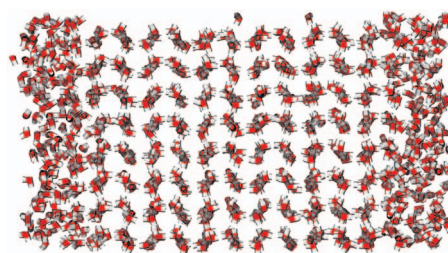


FIG. 13. (Color) Instantaneous configuration of the TIP4P/Ice system at 268 K at the end of a 5 ns run. Although the temperature is well below the melting point of the model, a quasiliquid layer is clearly present at the ice-vacuum interface. The plane that can be seen is the secondary prismatic plane. The plane exposed to the vacuum is the basal plane.

troscopy by Bluhm *et al.*²⁶ is presented and compared to the values obtained in this work (for δ_{true}). This comparison should be taken with a certain care since the criterion used to define a liquid layer may be different in experiment and in the simulations of this work. However, the agreement obtained is reasonable and the simulations seem to describe the experimental data qualitatively at least. It is not obvious at this stage whether the agreement for the liquidlike layer thickness obtained from computer simulation with that obtained from photoelectron spectroscopy experiments is accidental or is due to the presence of a common underlying observable. Further work is required to clarify this point. As it was already stated, the system sizes considered in this work allow us to obtain reliable values of the liquid layer thickness when it is not larger than about 10–12 Å. When the liquid layer becomes thicker (at the temperatures very close to the melting point) larger system sizes would be required.

In this work we have used a geometrical criterium to identify liquid and solid molecules. That presents the advantage of simplicity since the geometrical analysis of a certain snapshot allows to classify each molecule as liquid or solid. One may wonder whether a dynamic criterium could also be used to identify fluid and solid molecules. Although that makes the analysis more involved it is worth to explore this possibility. Here we shall present some results for the secondary prismatic plane of the TIP4P/2005 model. Simulations of bulk ice Ih (without interfaces) showed clearly that the plateau value of the mean square displacement was between 0.1 Å² (100 K) and 0.35 Å² (250 K). Practically no water molecule presented an individual mean square displacement larger than 1 Å². On the other hand we found that for TIP4P/2005 (which reproduces reasonably way the diffusion coefficient of real water), the mean square displacement in the bulk liquid was larger than 1 Å² after 400 ps (at least for temperatures above 200 K). Thus we decided to establish a simple dynamic criterium to classify the molecules as liquid or solid. A molecule will be classified as liquid if after 400 ps, its square displacement is larger than 1 Å² and will be solid otherwise. We do not pretend here to provide a quite elaborate dynamic definition but rather to establish a simple criterium. In Table VI the thickness of the quasiliquid layer determined by the dynamic criterium is provided. As it can be seen the thickness of the quasiliquid layer tends to zero at low temperatures. The thickness determined from the dy-

TABLE VI. Thickness of the liquid layer for TIP4P/2005 as obtained from the dynamic criteria δ_{dynamic} and from the geometric criteria δ_{apparent} and δ_{true} . The results were obtained for the secondary prismatic plane. δ_{dynamic} , δ_{apparent} , and δ_{true} are given in Å and the temperature is given in K.

Water model and plane	T	δ_{dynamic}	δ_{apparent}	δ_{true}
TIP4P/2005 (Secondary prism.)	249	8.9(7)	8.5(1.0)	6.0(1.2)
	247	7.5(5)	7.3(4)	4.8(6)
	230	3.9(3)	5.3(3)	2.8(5)
	200	1.5(3)	4.1(2)	1.6(4)
	180	1.2(6)	3.8(2)	1.3(4)
	140	0.5(1)	3.4(2)	0.9(4)
	100	0.1(1)	3.0(2)	0.5(4)
	30	0.0(1)	2.5(2)	0.0(2)

dynamic criteria is not identical to that obtained from the geometrical criteria. However, they are of the same order of magnitude and they agree reasonably well. Thus probably both geometrical and dynamic criteria can be used to identify liquid and solid molecules to determine the liquid layer thickness although in this work we have used extensively the geometric criteria.

Finally since a picture is worth a thousand words, let us finish by presenting an instantaneous configuration obtained for the TIP4P/Ice model at $T=268$ K in the basal plane. This is presented in Fig. 13. The picture shows a graphical evidence of the existence of a liquid layer at the free surface of ice.

IV. CONCLUSIONS

In this work we have reported on the results of computer simulation study of the formation of a liquid layer at the ice surface at the temperatures below the melting point. A slab of ice has been located in the middle of a large simulation box, and long MD runs have been performed, for different planes of ice exposed to vacuum. Three different planes considered: the secondary prismatic plane, the basal plane, and the primary prismatic plane. A tetrahedral orientational order parameter has been used to classify each water molecule within an instantaneous configuration as being liquidlike or solidlike. When the orientational order parameter was larger than the threshold value, set as equal to $q_t=0.91$, the molecule was regarded as an icelike. When the orientational order was smaller than the molecule was classified as a liquidlike. In this way the average number of liquidlike molecules was calculated, and the liquid layer thickness was estimated. Main findings of this work are as follows.

- There is a clear evidence that a liquid layer develops at the free surface of ice at the temperatures below the melting point.
- The appearance of liquid layers starts at different temperatures depending on the ice surface plane exposed to vacuum. It appears at the temperature of about -100 (with respect to the melting point) for the basal plane, at about -80 for the primary prismatic plane, and at about -70 for the secondary prismatic plane. The thickness of a liquid layer increases with temperature.

- At a given temperature the thickness of the liquid layer is larger for the basal plane than for the primary prismatic plane, and for the primary prismatic plane is larger than for the secondary prismatic plane.
- When the thicknesses of liquid layer for different water models are compared at the same degree of undercooling, then the value of the liquid layer thickness is practically the same for all water models.
- The thickness of the liquid layer seems to be of the order of about 10 Å at the temperatures up to $3-4$ K below the melting point. To determine the thickness at temperatures closer to the melting point, larger simulation cells and more accurate estimates of the melting point are needed.
- The thicknesses of liquid layers determined in this work seem to be of the same order of magnitude as determined by Bluhm *et al.*,²⁶ from photoelectron spectroscopy.

ACKNOWLEDGMENTS

This work was funded by Grant No. FIS2007-66079-C02-01 from the DGI (Spain), S-0505/ESP/0229 from the CAM, MTKD-CT-2004-509249 from the European Union, and 910570 from the UCM. M.M.C. would like to thank Universidad Complutense by the award of a Ph.D. grant.

- ¹M. Faraday, Proc. R. Soc. London **10**, 440 (1860).
- ²F. F. Abraham, Phys. Rep. **81**, 339 (1981).
- ³J. G. Dash, Contemp. Phys. **30**, 89 (1989).
- ⁴M. Bienfait, Surf. Sci. **272**, 1 (1992).
- ⁵J. Q. Broughton and G. H. Gilmer, J. Chem. Phys. **79**, 5119 (1983).
- ⁶D. Nenov, Prog. Cryst. Growth Charact. **9**, 185 (1984).
- ⁷J. W. M. Frenken and J. F. van der Veen, Phys. Rev. Lett. **54**, 134 (1985).
- ⁸J. W. M. Frenken, P. M. J. Maree, and J. F. Vanderveen, Phys. Rev. B **34**, 7506 (1986).
- ⁹A. Siavosh-Haghighi and D. L. Thompson, J. Phys. Chem. C **111**, 7980 (2007).
- ¹⁰F. Delogu, J. Phys. Chem. B **110**, 12645 (2006).
- ¹¹P. Carnevali, F. Ercolessi, and E. Tosatti, Phys. Rev. B **36**, 6701 (1987).
- ¹²B. Pluis, A. W. D. van der Gon, J. W. M. Frenken, and J. F. van der Veen, Phys. Rev. Lett. **59**, 2678 (1987).
- ¹³U. Tartaglino, T. Zykova-Timan, F. Ercolessi, and E. Tosatti, Phys. Rep. **411**, 291 (2005).
- ¹⁴H. Groenzin, I. Li, V. Buch, and M. J. Shultz, J. Chem. Phys. **127**, 214502 (2007).
- ¹⁵N. Materer, U. Starke, A. Barbieri, M. A. Vanhove, G. A. Somorjai, G. J. Kroes, and C. Minot, J. Phys. Chem. **99**, 6267 (1995).
- ¹⁶M. T. Suter, P. U. Andersson, and J. B. C. Pettersson, J. Chem. Phys. **125**, 174704 (2006).
- ¹⁷K. Bolton and J. B. C. Pettersson, J. Phys. Chem. B **104**, 1590 (2000).
- ¹⁸R. Rosenberg, Phys. Today **58**, 50 (2005).
- ¹⁹S. C. Colbeck, Am. J. Phys. **63**, 888 (1995).
- ²⁰S. C. Colbeck, Am. J. Phys. **65**, 488 (1997).
- ²¹M. J. Molina, The Chemistry of the Atmosphere: Its Impact on Global Change (Blackwell Scientific, Oxford, 1994).
- ²²Y. Li and G. A. Somorjai, J. Phys. Chem. C **111**, 9631 (2007).
- ²³J. G. Dash, H. Fu, and J. S. Wettlaufer, Rep. Prog. Phys. **58**, 115 (1995).
- ²⁴J. G. Dash, A. W. Rempel, and J. S. Wettlaufer, Rev. Mod. Phys. **78**, 695 (2006).
- ²⁵M. Elbaum, S. Lipson, and J. Dash, J. Cryst. Growth **129**, 491 (1993).
- ²⁶H. Bluhm, D. F. Ogletree, C. S. Fadley, Z. Hussain, and M. Salmeron, J. Phys.: Condens. Matter **14**, L227 (2002).
- ²⁷I. Golecki and C. Jaccard, J. Phys. Chem. Solids **11**, 4229 (1978).
- ²⁸D. Nason and N. H. Fletcher, J. Chem. Phys. **62**, 4444 (1975).

- ²⁹ H. Dosch, A. Lied, and J. H. Bilgram, *Surf. Sci.* **366**, 43 (1996).
- ³⁰ Y. Furukawa, M. Yamamoto, and T. Kuroda, *J. Cryst. Growth* **82**, 665 (1987).
- ³¹ D. Beaglehole and D. Nason, *Surf. Sci.* **96**, 357 (1980).
- ³² W. L. Jorgensen, J. Chandrasekhar, J. D. Madura, R. W. Impey, and M. L. Klein, *J. Chem. Phys.* **79**, 926 (1983).
- ³³ H. J. C. Berendsen, J. R. Grigera, and T. P. Straatsma, *J. Phys. Chem.* **91**, 6269 (1987).
- ³⁴ O. A. Karim, P. A. Kay, and A. D. J. Haymet, *J. Chem. Phys.* **92**, 4634 (1990).
- ³⁵ O. A. Karim and A. D. J. Haymet, *J. Chem. Phys.* **89**, 6889 (1988).
- ³⁶ S. C. Gay, E. J. Smith, and A. D. J. Haymet, *J. Chem. Phys.* **116**, 8876 (2002).
- ³⁷ T. Bryk and A. D. J. Haymet, *J. Chem. Phys.* **117**, 10258 (2002).
- ³⁸ G. T. Gao, X. C. Zeng, and H. Tanaka, *J. Chem. Phys.* **112**, 8534 (2000).
- ³⁹ E. Sanz, C. Vega, J. L. F. Abascal, and L. G. MacDowell, *Phys. Rev. Lett.* **92**, 255701 (2004).
- ⁴⁰ Y. Koyama, H. Tanaka, G. Gao, and X. C. Zeng, *J. Chem. Phys.* **121**, 7926 (2004).
- ⁴¹ C. Vega, E. Sanz, and J. L. F. Abascal, *J. Chem. Phys.* **122**, 114507 (2005).
- ⁴² R. G. Fernandez, J. L. F. Abascal, and C. Vega, *J. Chem. Phys.* **124**, 144506 (2006).
- ⁴³ J. Wang, S. Yoo, J. Bai, J. R. Morris, and X. C. Zeng, *J. Chem. Phys.* **123**, 036101 (2005).
- ⁴⁴ J. L. F. Abascal, R. G. Fernandez, L. MacDowell, E. Sanz, and C. Vega, *J. Mol. Liq.* **136**, 214 (2007).
- ⁴⁵ E. Sanz, C. Vega, J. L. F. Abascal, and L. G. MacDowell, *J. Chem. Phys.* **121**, 1165 (2004).
- ⁴⁶ L. Vrbka and P. Jungwirth, *J. Mol. Liq.* **134**, 64 (2007).
- ⁴⁷ J. L. F. Abascal and C. Vega, *J. Chem. Phys.* **123**, 234505 (2005).
- ⁴⁸ G. J. Kroes, *Surf. Sci.* **275**, 365 (1992).
- ⁴⁹ Y. Furukawa and H. Nada, *J. Phys. Chem. B* **101**, 6167 (1997).
- ⁵⁰ H. Nada and Y. Furukawa, *Appl. Surf. Sci.* **121**, 445 (1997).
- ⁵¹ M. A. Carignano, P. B. Shepson, and I. Szleifer, *Mol. Phys.* **103**, 2957 (2005).
- ⁵² T. Ikeda-Fukazawa and K. Kawamura, *J. Chem. Phys.* **120**, 1395 (2004).
- ⁵³ M. A. Carignano, P. B. Shepson, and I. Szleifer, *Chem. Phys. Lett.* **436**, 99 (2007).
- ⁵⁴ H. Nada and J. P. J. M. van der Eerden, *J. Chem. Phys.* **118**, 7401 (2003).
- ⁵⁵ F. Paesani and G. A. Voth, *J. Phys. Chem. C* **112**, 324 (2008).
- ⁵⁶ S. Picaud, *J. Chem. Phys.* **125**, 174712 (2006).
- ⁵⁷ C. Vega, M. Martin-Conde, and A. Patrykiewicz, *Mol. Phys.* **104**, 3583 (2006).
- ⁵⁸ C. McBride, C. Vega, E. Sanz, L. G. MacDowell, and J. L. F. Abascal, *Mol. Phys.* **103**, 1 (2005).
- ⁵⁹ G. E. Norman and V. V. Stegailov, *Dokl. Phys.* **47**, 667 (2002).
- ⁶⁰ G. E. Norman and V. V. Stegailov, *Mol. Simul.* **30**, 397 (2004).
- ⁶¹ J. Frenkel, *Kinetic Theory of Liquids* (Oxford University Press, New York, 1946).
- ⁶² V. F. Petrenko and R. W. Whitworth, *Physics of Ice* (Oxford University Press, Oxford, 1999).
- ⁶³ J. D. Bernal and R. H. Fowler, *J. Chem. Phys.* **1**, 515 (1933).
- ⁶⁴ L. Pauling, *J. Am. Chem. Soc.* **57**, 2680 (1935).
- ⁶⁵ V. Buch, P. Sandler, and J. Sadlej, *J. Phys. Chem. B* **102**, 8641 (1998).
- ⁶⁶ D. Van Der Spoel, E. Lindahl, B. Hess, G. Groenhof, A. E. Mark, and H. J. C. Berendsen, *J. Comput. Chem.* **26**, 1701 (2005).
- ⁶⁷ J. P. Ryckaert, G. Ciccotti, and H. J. C. Berendsen, *J. Comput. Phys.* **23**, 327 (1977).
- ⁶⁸ H. J. C. Berendsen and W. F. van Gusteren, in *Molecular Liquids-Dynamics and Interactions*, Proceedings of the NATO Advanced Study Institute on Molecular Liquids (Reidel, Dordrecht, 1984), pp. 475–500.
- ⁶⁹ U. Essmann, L. Perera, M. L. Berkowitz, T. Darden, H. Lee, and L. G. Pedersen, *J. Chem. Phys.* **103**, 8577 (1995).
- ⁷⁰ S. Nosé, *Mol. Phys.* **52**, 255 (1984).
- ⁷¹ W. G. Hoover, *Phys. Rev. A* **31**, 1695 (1985).
- ⁷² M. Parrinello and A. Rahman, *J. Appl. Phys.* **52**, 7182 (1981).
- ⁷³ S. Nosé and M. L. Klein, *Mol. Phys.* **50**, 1055 (1983).
- ⁷⁴ J. Alejandro, F. Bresme, M. Gonzalez-Melchor, and F. del Rio, *J. Chem. Phys.* **126**, 224511 (2007).
- ⁷⁵ C. Vega and E. de Miguel, *J. Chem. Phys.* **126**, 154707 (2007).
- ⁷⁶ H. Nada and Y. Furukawa, *J. Cryst. Growth* **283**, 242 (2005).
- ⁷⁷ M. Chaplin (<http://www.lsbu.ac.uk/water/>).
- ⁷⁸ M. Matsumoto, *J. Chem. Phys.* **126**, 054503 (2007).
- ⁷⁹ J. R. Errington and P. G. Debenedetti, *Nature (London)* **409**, 318 (2001).
- ⁸⁰ N. Giovambattista, P. G. Debenedetti, F. Sciortino, and H. E. Stanley, *Phys. Rev. E* **71**, 061505 (2005).
- ⁸¹ T. Head-Gordon and M. E. Johnson, *Proc. Natl. Acad. Sci. U.S.A.* **103**, 7973 (2006).
- ⁸² P. Wernet, D. Nordlund, U. Bergmann, M. Cavalleri, M. Odelius, H. Ogasawara, L. A. Naslund, T. K. Hirsch, L. Ojamae, P. Glatzel, L. G. M. Pettersson, and A. Nilsson, *Science* **304**, 995 (2004).
- ⁸³ Y. I. Jhon, K. T. No, and M. S. Jhon, *J. Phys. Chem. B* **111**, 9897 (2007).